Supporting Information

Modulating excited state via diversified electron-donating units in MR-TADF emitters: a theoretical exploration of structure-property relationships

Zhu Chang,[1] Rajat Walia,[1] Dandan Zhang,[2] Xian-Kai Chen[1,3] and Jiaqi Li[1,*]

[1]Institute of Functional Nano and Soft Materials (FUNSOM), Soochow University, Suzhou, Jiangsu, 215123, P. R. China.

[2]Soochow College, Soochow University, Suzhou, Jiangsu, 215123, P. R. China.

[3]State Key Laboratory of Bioinspired interfacial Materials Science, Soochow University, Suzhou, Jiangsu 215123, P.R. China

Email: jqli0926@suda.edu.cn

Contents

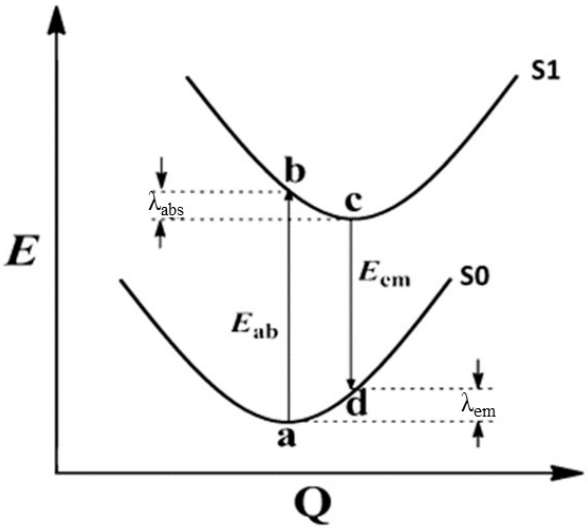

$$\lambda_{em} = \sum_{j \in gs} \lambda_j = \sum_{j \in gs} \hbar w_j HR_j$$

$$\lambda_{abs} = \sum_{j \in es} \lambda_j = \sum_{j \in es} \hbar w_j HR_j$$

Fig. S1 Schematic diagram of the potential energy surfaces and computational details for relaxation energies. λ_{em} is defined as the energy change from the geometric relaxation of the S_1 state to the equilibrium configuration of the S_0 state.

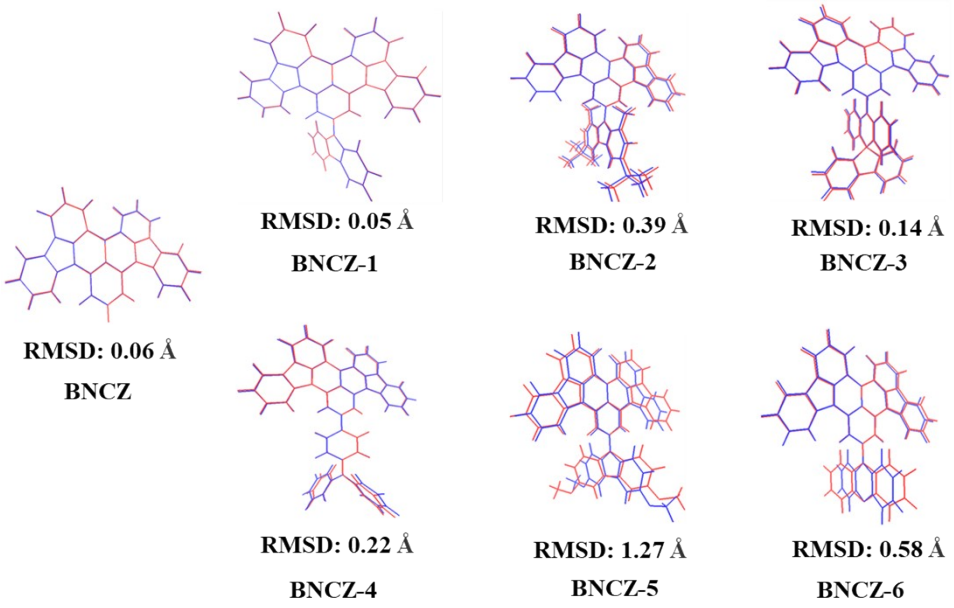

Fig. S2 Diagram of geometry comparisons between S_0 and S_1 states together with the calculated RMSD values for the studied molecules (the structures at S_0 and S_1 states are

depicted in red and blue, respectively) with PBE0/6-31G(d,p) method.

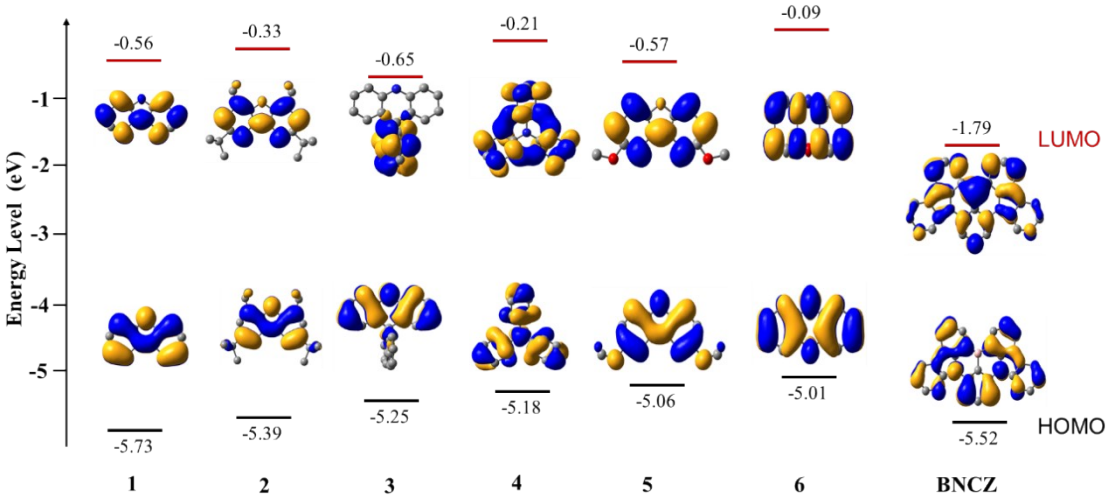

Fig. S3 Calculated FMOs electron distributions and energy levels of donor units and BNCZ segment at PBE0/6-31G(d,p).

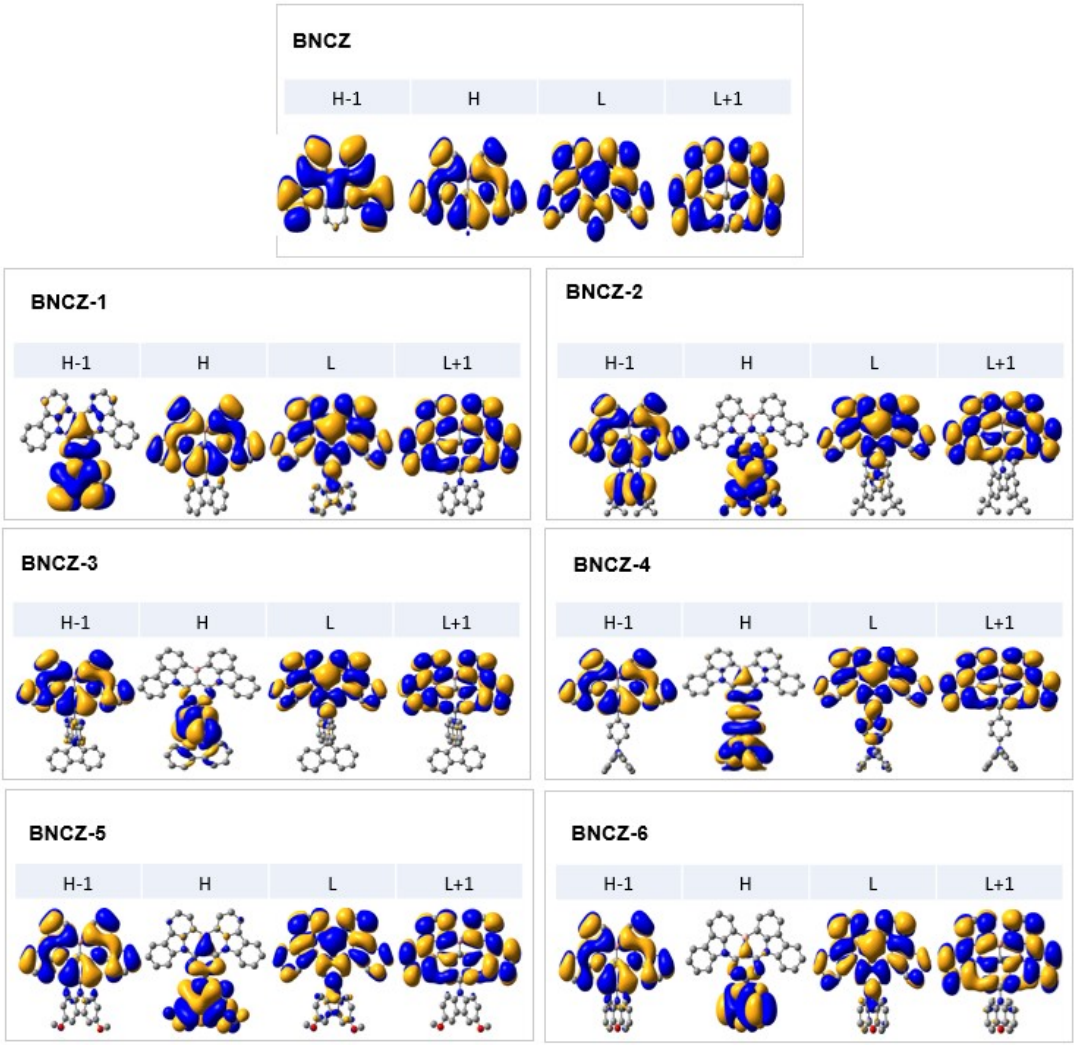

Fig. S4 FMOs spatial distributions of the investigated molecules at PBE0/6-31G(d,p).

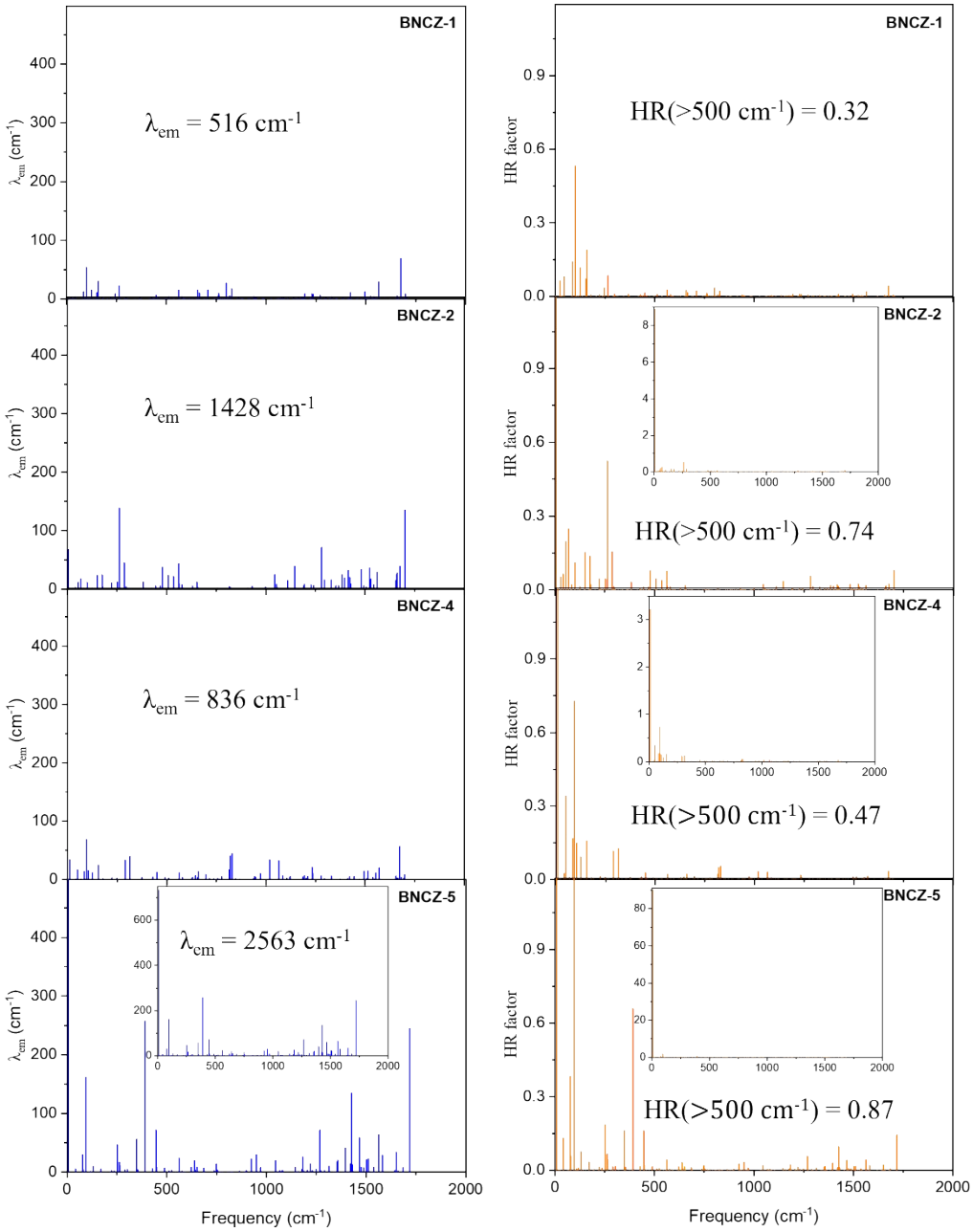

Fig. S5 Calculated relaxation energy (λ_{em}) and Huang-Rhys (HF) factor versus the normal mode frequencies for the investigated molecules relevant to $S_1 \rightarrow S_0$ process.

Table S1. The calculated HOMO energy levels (eV) in dichloromethane solution with different DFT functionals.

	BNCZ-3	BNCZ-6
B3LYP	-5.18	-4.87
PBE0	-5.46	-5.16
PBE38	-5.96	-5.64
M062X	-6.55	-6.18
ωB97XD	-6.46	-6.29
Exp.	-5.44[a]	-5.08[b]

[a] refers to [1,2]; [b] refers to [3].

Table S2. Absorption energy (E_{abs}), emission energy (E_{em}) and energy gap between singlet and triplet states (ΔE_{ST}) of BNCZ-3 and BNCZ-6, calculated by 6-31G(d,p) for TDDFT and def2-TZVP for STEOM-DLPNO-CCSD.as well as experimental data for BNCZ-3 and BNCZ-6.

	BNCZ-3			BNCZ-6		
	E_{abs} (S_0---S_1)	E_{em} (S_1---S_0)	ΔE_{ST}	E_{abs} (S_0---S_1)	E_{em} (S_1---S_0)	ΔE_{ST}
CCSD	2.75	2.69	0.11	2.79	2.78	0.09
PBE0	2.77	2.56	0.26	2.51	2.18	0.06
Cam-B3LYP	3.28	3.17	0.56	3.32	3.23	0.56
B3LYP	2.60	2.41	0.14	2.34	2.03	0.04
PBE38	3.15	3.04	0.56	2.99	2.65	0.37
M062X	3.27	3.17	0.38	3.27	3.18	0.38
ωB97XD	3.06	2.95	0.40	3.15	3.07	0.40
EXP	2.68[a]	2.59[a]	0.15[a]	2.69[b]	2.06[b]	0.12[b]

[a] refers to [1,2]; [b] refers to [3].

Table S3. Bond length (Å) at S_0 optimized geometry by using PBE0 functionals as well as experimental data for BNCZ-6, the standard deviation σ is calculated by the formula $\sigma = \sqrt{\frac{1}{N}\sum_{i=1}^{N}(x_i - x_{exp})^2}$.

BNCZ-6	Exp. [a]
1.35380	1.38970
1.39752	1.39666
1.42961	1.42374
1.42473	1.42374
1.39976	1.39666
1.36714	1.38970
1.40544	1.39459
1.39854	1.38835
1.3987	1.39835
1.53084	1.53803
1.54321	1.53975
1.54626	1.53803
1.39443	1.39835
1.39091	1.38836
1.39966	1.39459
1.42814	1.41111
1.40082	1.3953
1.35995	1.39214
1.38956	1.39668
1.37618	1.38834
1.39519	1.39263
1.44385	1.44505
1.38560	1.38927
1.38704	1.39712
1.384	1.39321
1.4104	1.40738
1.40781	1.40666
1.4116	1.41609

	1.42814	1.41111
	1.40082	1.3953
	1.35995	1.39214
	1.38956	1.39668
	1.37618	1.38834
	1.39519	1.39263
	1.44385	1.44505
	1.38560	1.38927
	1.38704	1.39712
	1.384	1.39321
	1.4104	1.40738
	1.40781	1.40666
	1.4116	1.41609
	1.435	1.42
	1.40184	1.40433
	1.38808	1.39603
	1.3872	1.39442
	1.37476	1.38724
	1.38374	1.39359
	1.37503	1.38427
	1.39048	1.37112
	1.38964	1.37112
	1.3737	1.38427
	1.38161	1.39359
	1.3746	1.38724
	1.38469	1.39442
	1.38728	1.39603
	1.40285	1.40433
	1.38662	1.40366
	1.39452	1.40366
σ	0.011	

[a] refers to [3].

Table S4. Calculated excited-states dominant orbital transitions and character assignments for the investigated molecules with CASSCF method.

Mol.	State	Main configuration	Transition character
BNCZ	S_1	98.4% ($\Psi_H \rightarrow \Psi_L$)	SRCT
	T_1	76.9% ($\Psi_H \rightarrow \Psi_L$)	SRCT
		10.0% ($\Psi_{H-1} \rightarrow \Psi_L$)	
	T_2	76.6% ($\Psi_H \rightarrow \Psi_L$)	SRCT
		10.1% ($\Psi_{H-1} \rightarrow \Psi_L$)	
BNCZ-1	S_1	73.5% ($\Psi_H \rightarrow \Psi_L$)	SRCT + LRCT
		16.5% ($\Psi_{H-1} \rightarrow \Psi_{L+1}$)	
	T_1	63.8% ($\Psi_H \rightarrow \Psi_{L+1}$)	SRCT + LRCT
		33.6% ($\Psi_{H-1} \rightarrow \Psi_L$)	
	T_2	88.6% ($\Psi_H \rightarrow \Psi_L$)	LRCT + SRCT
		8.3% ($\Psi_{H-1} \rightarrow \Psi_{L+1}$)	
BNCZ-2	S_1	73.6% ($\Psi_{H-1} \rightarrow \Psi_L$)	SRCT + LRCT
		15.1% ($\Psi_H \rightarrow \Psi_{L+1}$)	
	T_1	65.9% ($\Psi_{H-1} \rightarrow \Psi_{L+1}$)	SRCT + LRCT
		31.4% ($\Psi_H \rightarrow \Psi_L$)	
	T_2	90.2% ($\Psi_{H-1} \rightarrow \Psi_L$)	LRCT + SRCT
		7.20% ($\Psi_H \rightarrow \Psi_{L+1}$)	
BNCZ-3	S_1	60.9% ($\Psi_{H-1} \rightarrow \Psi_L$)	SRCT + LRCT
		18.1% ($\Psi_H \rightarrow \Psi_L$)	
	T_1	41.4% ($\Psi_{H-1} \rightarrow \Psi_{L+1}$)	SRCT + LRCT
		38.7% ($\Psi_H \rightarrow \Psi_L$)	
		18.8% ($\Psi_H \rightarrow \Psi_{L+1}$)	
	T_2	77.0% ($\Psi_{H-1} \rightarrow \Psi_L$)	LRCT + SRCT
		9.4% ($\Psi_H \rightarrow \Psi_L$)	
		10.3% ($\Psi_{H-1} \rightarrow \Psi_{L+1}$)	
BNCZ-4	S_1	75.9% ($\Psi_{H-1} \rightarrow \Psi_L$)	SRCT + LRCT
		13.8% ($\Psi_H \rightarrow \Psi_{L+1}$)	
	T_1	89.3% ($\Psi_H \rightarrow \Psi_L$)	SRCT + LRCT
	T_2	87.1% ($\Psi_{H-1} \rightarrow \Psi_L$)	LRCT + SRCT

		6.8% ($\Psi_H \rightarrow \Psi_{L+1}$)	
BNCZ-5	S_1	97.1% ($\Psi_{H-1} \rightarrow \Psi_L$)	LRCT+ SRCT
	T_1	100% ($\Psi_H \rightarrow \Psi_{L+1}$)	LRCT+ SRCT
	T_2	97.1% ($\Psi_{H-1} \rightarrow \Psi_L$)	LRCT + SRCT
BNCZ-6	S_1	97.7% ($\Psi_H \rightarrow \Psi_L$)	LRCT
	T_1	65.0% ($\Psi_{H-1} \rightarrow \Psi_{L+1}$)	SRCT + LRCT
		33.0% ($\Psi_H \rightarrow \Psi_L$)	
	T_2	91.1% ($\Psi_{H-1} \rightarrow \Psi_L$)	SRCT + LRCT
		7.3% ($\Psi_H \rightarrow \Psi_{L+1}$)	

Table S5. Calculated excited-state energy levels (E_{S1}, E_{T1}, and E_{T2}, eV), singlet–triplet energy gaps ($\Delta E_{S1\text{-}T1}$, $\Delta E_{S1\text{-}T2}$, eV), T_1-T_2 energy gaps ($\Delta E_{T1\text{-}T2}$, eV), RISC reorganization energies ($\lambda_{T1\text{-}S1}$, $\lambda_{T2\text{-}S1}$, eV), SOC constants ($SOC_{T1\text{-}S1}$, $SOC_{T2\text{-}S1}$, cm^{-1}), and k_{RISC} (s^{-1}) for the investigated molecules at STEOM-DLPNO-CCSD/def2-TZVP.

Mol.	BNCZ	BNCZ-1	BNCZ-2	BNCZ-3	BNCZ-4	BNCZ-5	BNCZ-6
E_{S1}	2.73	2.76	2.63	2.62	2.76	2.60	2.54
	2.75[a]			2.66[b]			2.64[c]
E_{T1}	2.51	2.47	2.46	2.51	2.66	2.55	2.45
	2.60[a]			2.51[b]			2.52[c]
E_{T2}	2.55	2.48	2.48	2.52	2.75	2.85	2.68
$\Delta E_{S1\text{-}T1}$	0.22	0.29	0.17	0.11	0.10	0.05	0.09
Exp.	0.15			0.15			0.12
$\Delta E_{S1\text{-}T2}$	0.18	0.28	0.15	0.10	0.01	-0.25	-0.14
$\Delta E_{T2\text{-}T1}$	0.04	0.01	0.02	0.01	0.09	0.30	0.23
$\lambda_{T1\text{-}S1}$	0.03	0.22	0.30	0.16	0.03	0.26	0.11
$\lambda_{T2\text{-}S1}$	0.31	0.31	0.38	0.37	0.15	0.08	0.24
$SOC_{T1\text{-}S1}$	0.07	0.05	0.04	0.05	0.06	0.06	0.07
$SOC_{T2\text{-}S1}$	0.29	0.20	0.23	0.31	0.38	0.29	0.33
k_{RISC}	0.32×10^4	0.16×10^3	0.63×10^4	0.84×10^5	4.80×10^5	0.45×10^5	0.10×10^6
Exp.	1.20×10^{4a}			7.36×10^{5b}			2.06×10^{6c}

[a] refers to [3]; [b] refers to [1,2]; [c] refers to [3].

Table S6. Calculated emission oscillator strength (*f*), transition dipole moment (μ, D), and fluorescence radiative rate (k_r, s^{-1}) at STEOM-DLPNO-CCSD/def2-TZVP.

Mol.	BNCZ	BNCZ-1	BNCZ-2	BNCZ-3	BNCZ-4	BNCZ-5	BNCZ-6
f	0.52	0.48	0.48	0.50	0.47	0.13	0.05
μ	2.73	2.63	2.65	2.71	2.63	1.35	0.87
k_r	1.68×10^8	1.58×10^8	1.44×10^8	1.49×10^8	1.55×10^8	3.81×10^7	1.40×10^7
Exp.	1.17×10^{8a}			1.26×10^{8b}			1.0×10^{7c}

[a] refers to [3]; [b] refers to [1,2]; [c] refers to [3].

References

1 X. Song, S. Shen, S. Zou, F. Guo, Y. Wang, S. Gao, Y. Zhang, Efficient narrowband organic light-emitting devices based on multi-resonance TADF emitters with secondary donor. *Chem. Eng. J.*, 2023, **467**, 143557.

2 Q. Wu, J. Li, D. Liu, Y. Mei, B. Liu, J. Wang, M. Xu, Y. Li, Dual emission from donor-modified MR-TADF emitter: Evidence for coexistence of TICT and MR excited states. *Dyes Pigments*, 2023, **217**, 111421.

3 Z. Huang, H. Xie, J. Miao, Y. Wei, Y. Zou, T. Hua, X. Cao, C. Yang, Charge transfer excited state promoted multiple resonance delayed fluorescence emitter for high-performance narrowband electroluminescence. *J. Am. Chem. Soc.*, 2023, **145**, 12550-12560.